GANIL

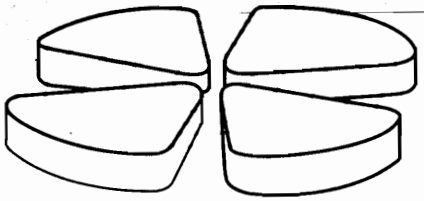

A determination of the ^{6}He+p interaction potential

A. de Vismes[a], P. Roussel-Chomaz[a], W. Mittig[a], A. Pakou[a,b], N. Alamanos[c], F. Auger[c], J-C. Angélique[d], J. Barrette[e], A.V. Belozyorov[f], C. Borcea[a,g], W.N. Catford[d,h], M-D. Cortina-Gil[i], Z. Dlouhy[j], A. Gillibert[c], V. Lapoux[c], A. Lepine-Szily[k], S.M. Lukyanov [f], F. Marie[c], A. Musumarra[c,1], F. de Oliveira[a], N.A. Orr[d], S. Ottini-Hustache[c], Y.E. Penionzhkevich[f], F. Sarazin[a,2], H. Savajols[a], N. Skobelev[f]

Submitted for publication in Physics Letters B

GANIL P 00 50

A determination of the ^{6}He+p interaction potential

A. de Vismes[a], P. Roussel-Chomaz[a], W. Mittig[a], A. Pakou[a,b], N. Alamanos[c], F. Auger[c], J-C. Angélique[d], J. Barrette[e], A.V. Belozyorov[f], C. Borcea[a,g], W.N. Catford[d,h], M-D. Cortina-Gil[i], Z. Dlouhy[j], A. Gillibert[c], V. Lapoux[c], A. Lepine-Szily[k], S.M. Lukyanov [f], F. Marie[c], A. Musumarra[c,1], F. de Oliveira[a], N.A. Orr[d], S. Ottini-Hustache[c], Y.E. Penionzhkevich[f], F. Sarazin[a,2], H. Savajols[a], N. Skobelev[f]

[a] *GANIL (DSM/CEA, IN2P3/CNRS), BP 5027, 14076 Caen Cedex 5, France*
[b] *Department of Physics, The University of Ioannina, 45110 Ioannina, Greece*
[c] *CEA/DSM/DAPNIA/SPhN, Saclay, 91191 Gif-sur-Yvette Cedex, France*
[d] *LPC, IN2P3/CNRS, ISMRa et Université de Caen, F-14050 Caen, Cedex, France*
[e] *McGill University, 845 Sherbrooke St., Montreal, Quebec, H3A 3R1, Canada*
[f] *FLNR,JINR Dubna, P. O. Box 79, 101 000 Moscow, Russia*
[g] *Inst. Atomic Physics, P.O. Box MG6, Bucharest, Romania*
[h] *Department of Physics, University of Surrey, Guildford, Surrey GU2 7XH, United Kingdom*
[i] *Dpto Fisica de Particulas, Universidad Santiago de Compostela, 15706 Santiago de Compostela, Spain*
[j] *Nuclear Physics Institute, ASCR, 25068 Rez, Czech Republic*
[k] *IFUSP-Universidade de São Paulo, C.P. 66318, 05389-970 São Paulo, Brazil*

[1] present address: INFN-Laboratori Nazionali del Sud, Via S. Sofia 44, 95123 Catania Italy
[2] present address: Department of Physics and Astronomy, Edinburgh EH9 3JZ, Scotland, UK

Abstract

The reaction cross section for the halo nucleus ^{6}He on hydrogen has been measured at 36 MeV/nucleon using the transmission method and a value of σ_R=409±22mb was obtained. A coherent analysis within a microscopic model of this result in conjunction with (p, p) and (p, n) angular distributions has allowed the interaction potential to be uniquely determined. This analysis also allowed the ^{6}He density distribution to be explored.

PACS number(s): 25.60.Dz,25.60.Bx,25.60.Lg

KEYWORDS : reaction cross section, elastic proton scattering, charge exchange, halo nuclei, microscopic calculations.

Proton-nucleus elastic scattering has been studied extensively and both phenomenological and microscopic potential models have been developed [1-6]. In particular, a large amount of experimental data has been successfully interpreted through such models with at most the adjustment of only a few parameters [3-11].

With the advent of radioactive beam facilities, elastic scattering measurements have been extended to neutron-rich nuclei close to the drip lines (see, for example, refs [12-15]). However, because of the low beam intensities, such studies often span a limited angular range and cannot probe unambiguously the potential, partly because the effects of the potential cannot be disentangled from the little known density distribution of these nuclei. In this context, reaction cross-section measurements are a valuable tool. Absorbing processes affect the elastic scattering angular distribution and thus reaction cross sections can place restrictions on the amount of absorption, as represented by the imaginary potential [16, 17]. In contrast, (p,n) reactions leading to isobaric analog states (IAS) can be used to probe the isovector part of the potential. Consequently, the simultaneous analysis of elastic proton scattering, (p,n) charge exchange and reaction cross section data can provide strong constraints on the interaction potential for neutron-rich nuclei and tell us something about their structure.

We have previously reported results on the proton elastic scattering and (p,n) charge exchange reaction on ^{6}He [12, 18]. It was shown in [12] that these first elastic scattering data are not well reproduced by standard proton-nucleus potentials derived from elastic scattering measurements on stable nuclei. A good description of the data was obtained by either a reduction of the amplitude of the real potential or an important increase of the imaginary potential. A description of the charge exchange reaction leading to the IAS of ^{6}He favored this last option [18]. A more quantitative conclusion was not posssible partly because of the limited angular range, (θ_{cm}=15-40 deg), of the elastic scattering data reported in [12]. Very recently a new elastic scattering angular distribution measurement [13], spanning a broader range of angles (θ_{cm}=10-80 deg), was obtained using the MUST detector array [19]. The analysis of the p-^{6}He interaction reported

here uses these new data. Additionally, as described here, a reaction cross section measurement on a hydrogen target has been undertaken.

We report in this Letter on the coherent analysis of three data sets - (p,p) elastic scattering [13], (p,n) charge exchange [18] and the present reaction cross section measurement- within a microscopic framework. The aim of this work was to achieve a better description of the interaction potential for ^{6}He. The experimental details concerning the elastic scattering and charge exchange reactions, have been reported elsewhere [12, 13, 18]. The p+^{6}He reaction cross section forms part of a series of measurements for light stable and neutron-rich nuclei which will be published in the near future [20]. The experimental procedure is thus only briefly summarized here.

The ^{6}He beam was produced by fragmentation of a 60 MeV/nucleon ^{48}Ca primary beam delivered by the GANIL accelerator complex, and incident on a Be production target, backed by Ta. The secondary ions were subsequently selected using the spectrometer LISE [21].

The reaction cross section, σ_R, was measured using the transmission method [22]. In such a measurement, the attenuation of the ^{6}He beam passing through the target is measured and the reaction probability is given by

$$P_R = \frac{N_{reac}}{N_{inc}} = 1 - \frac{N_f}{N_i} = 1 - \exp\left(-\sigma_R \frac{Nd}{A} e\right) \quad (1)$$

where σ_R is the reaction cross section, d is the target density, N is the Avogadro number, A is the target mass number and e is the thickness of the target. In the present measurement, liquid hydrogen targets (35 and 70 mg/cm^2 thick) were used.

By measuring the number of incident and transmitted ions, the reaction cross section may be directly determined. The incident ^{6}He ions (36.2 MeV/nucleon), were identified by their characteristic energy loss and time-of-flight with respect to the cyclotron RF, using an ionization chamber and a microchannel plate timing detector, placed upstream of the hydrogen target.

The transmitted ions were identified using a large area (50x50 mm^2) telescope, set up 6.5 cm downstream of the target. The telescope was composed of a thin (500μm) position sensitive Si detector, a Si(Li) detector (3500μm) and a thick stopping CsI scintillator (4.5 cm)[23].

The measured reaction cross section, σ_R=409$\pm$22 mb, is 10% higher than the empirical prediction of Kox et al.(σ_R=365 mb) [24]. The Kox formula reproduces σ_R well for a wide variety of nuclei, over a broad energy range, and as such the observed enhancement is consistent with the halo structure of ^{6}He.

In order to study the interaction potential and the effect of the density distribution of ^{6}He in a consistent manner, calculations using the Jeukenne, Lejeune and Mahaux approach (JLM) [1] of the nuclear interaction potential were undertaken to fit simultaneously the reaction cross section and the angular distributions derived from the elastic scattering [13] and charge exchange reactions [18]. Calculations were performed within a microscopic DWBA approach, in

which entrance and exit-channel optical potentials were calculated consistently using the JLM energy and density dependent interaction. The starting point for computing the JLM potentials, is the Brueckner-Hartree-Fock approximation and the Reid hard core nucleon-nucleon interaction which describes, for energies up to 160 MeV, the energy and density dependence of the isoscalar, isovector and Coulomb components of the complex optical potential in infinite matter.

The optical potential of a finite nucleus is obtained by using the local density approximation (LDA), that is by substituting the nuclear matter density by the density distribution of the nucleus. The JLM central potential has been extensively studied by Mellema et al. [8] and Petler et al. [9]. It has been particularly successful in describing elastic proton and neutron scattering for light stable nuclei, provided that the imaginary potential is adjusted slightly by a normalization factor (λ_w) of around 0.8. In the following, this will be referred to as the standard normalization.

As noted earlier, elastic proton scattering brings valuable information on the nuclear interaction potential, while reaction cross sections provide complementary constraints on the imaginary part. As may be seen in Table 1, where calculated reaction cross sections for ^{6}He + p at 36.2 MeV are displayed for various potentials, variations in the normalization factor for the real potential has little effect, whereas the reaction cross section varies linearly with the amplitude of the imaginary potential. As such, the normalization factor for the imaginary potential derived from elastic scattering can be corroborated using the reaction cross section. Table 1 also demonstrates that the reaction cross section is sensitive to the isovector part of the interaction potential. Previous work has shown that even for such neutron-rich nuclei as ^{6}He, elastic scattering is almost not sensitive to the isovector part of the potential[25], as opposed to the (p,n) charge exchange reaction to the IAS [26].

The analysis subsequently proceeded by iterative fitting of the elastic scattering angular distribution, the reaction cross section and the (p,n) angular distribution. An input to these calculations is the ^{6}He nucleus density distribution. At first, densities determined via a shell model approach [27] were employed. The best fit of the elastic scattering data obtained with these densities is presented in Fig 1a (solid line), and was obtained with λ_v=0.85 and λ_w=0.59 (χ^2=1.12, see Table 2), irrespective of the isovector component. The latter was adjusted through fits to the (p,n) angular distribution resulting in a normalization of λ_{isov}=1.4 (Fig 2a). Using the potential determined in this manner (λ_v=0.85, λ_w=0.59 and λ_{isov}=1.4), a reaction cross section of 320mb was predicted, which is much lower than the measured value. An increase in the imaginary part of the potential is required to reproduce the reaction cross section measurement. From Table 1 it is seen that the imaginary part should be increased to λ_w=0.85 to reproduce the experimental reaction cross section. The elastic scattering was then re-examined, by fixing the imaginary normalization factor to λ_w=0.85 and by varying the real part of the optical potential. The

constrained fit, (χ^2=3.96), was obtained for λ_v=0.88 (Fig 1a, dashed line) and represents an adequate compromise for a simultaneous description of the three sets of data.

The sensitivity to the density distribution was studied by repeating the above iterative procedure for the following theoretical halo density distributions:

- A density calculated from a three-body cluster model [28] with a RMS radius similar to the previous shell model one.

- A density distribution calculated from an extended three-body cluster model [29] for four different descriptions: a) a pure three cluster model α+n+n; b) a three cluster model with the inclusion of a t+t component; c) an extended three cluster [3N+N]+n+n model; and d) an extended three cluster model with a t+t component.

The RMS radii of all the above densities are listed in Table 2. The details of the calculations are also presented in the same Table. The (p,n) data were found to be compatible with an isovector adjustment of λ_{isov}=1.4 for all the densities (Fig. 2b). The best fits as well as the constrained fits, obtained with the reaction cross section constraint on the imaginary part of the potential, are shown in Figures 1b and 1c, for the densities of Ref. [28] and [29] respectively. The quality of the fits, as noted by the χ^2 values in Table 2, is slightly in favour of the cluster model density distributions of Arai, Suzuki and Lovas. However neither the elastic scattering nor the reaction cross section can distinguish between the four different descriptions (Table 2) of ^{6}He in this model.

It should be stressed that the normalization adjustments for both the real and imaginary parts of the optical potential depend on the density distribution of the nucleus. On the other hand, no such dependence within the experimental uncertainties is apparent in Fig 2b, where calculations for the (p,n) reaction with various halo densities are compared with the measured angular distribution and show good compatibility, irrespective of the choice of density and of the real and imaginary potentials, with an isovector adjustment of λ_{isov}=1.4.

In summary, the reaction cross section p+ ^{6}He has been measured in inverse kinematics at 36 MeV. This result has been incorporated into a consistent microscopic description of earlier (p,p) and (p,n) angular distribution measurements. It was shown that the JLM potential can describe adequately ^{6}He (p,p) elastic scattering, (p,n) charge exchange and the reaction cross section measurement with an imaginary potential close to the standard one for light stable nuclei. The best description of the ensemble of the data was obtained when the imaginary part of the potential is increased by roughly 10%, and the real part is decreased by roughly 10% in comparison with the standard normalization factors. The need to reduce the real part of the potential was noticed before in the case of nucleus–nucleus elastic scattering involving weakly bound stable nuclei, and was attributed to coupling to the continuum [11,30]. As to the isovector part of the interaction potential, both the reaction cross section and the (p,n) charge exchange angular distribution required an increase of about 40% (λ_{isov}=1.4) with respect to the standard normalization, which is smaller

than that for stable nuclei (λ_{isov}=2.5) [31].

It is important to note that such conclusions could be drawn only because a wide range of data was available on the same nucleus at the same beam energy, thus enabling the effects of the different parts of the interaction potential to be disentangled.

1 References

[1] J. P. Jeukenne, A. Lejeune, C. Mahaux, Phys. Rev C 16 (1977) 80.

[2] F. A. Brieva, J. R. Rook, Nucl. Phys. A307 (1978) 493.

[3] R. L. Varner et al.,Phys. Rep. 201 (1991) 57.

[4] F. D. Becchetti, G. W. Greenlees, Phys. Rev 182 (1969) 1190.

[5] E. D. Couper et al., Phys. Rev. C 47 (1993) 297.

[6] S. Hama et al., Phys. Rev C 41 (1990) 2737.

[7] F. Petrovich et al., Nucl. Phys. A 563 (1993) 387.

[8] S. Mellema et al., Phys. Rev C 28 (1983) 2267.

[9] J. S. Petler et al., Phys. Rev C 32 (1985) 673.

[10] F. S. Dietrich et al., Phys. Rev. Lett 51 (1983) 2267.

[11] G. R. Satchler and W.G. Love, Phys. Rep 55 (1979) 184.

[12] M. D. Cortina-Gil et al., Phys. Lett B 401(1997) 9.

[13] F. Auger et al., AIP Conference proceedings 495, p 13 ENPE 99 Seville Spain, June 21-26 1999 and A. Lagoyannis et al., submitted for publication.

[14] A. A. Korsheninnikov et al., Phys. Lett. B 316 (1993) 38.

[15] A. A. Korsheninnikov et al., Nucl. Phys. A 617 (1997) 45.

[16] A. M. Sawkes et al., Phys. Rev C 13 (1976) 451.

[17] M. C. Mermaz, Phys. Rev C 50 (1994) 2620.

[18] M.D. Cortina-Gil et al., Nucl. Phys. A 641 (1998) 263.

[19] Y. Blumenfeld, et al., NIM in Physics Research A 421 (1999) 471.

[20] Anne de Vismes et al., in preparation; and PhD Thesis, University of Caen, France 2000.

[21] R. Anne et al., Nucl. Inst. Meth. A 257 (1985) 215.

[22] R. F. Carlson et al., Nucl. Inst. Meth. 123 (1975) 509.

[23] R. L. Cowin et al., Nucl. Inst. Meth. A 423 (1999) 75.

[24] S. Kox et al., Phys. Rev. 35 (1987) 1678.

[25] M-D Cortina-Gil, private communication.

[26] F. S. Dietrich and F. Petrovich, in Proc. of Neutron-Nucleus Collisions -A Probe of Nuclear Structure, eds J. Rapaport, AIP Conference Proceedings, no 124 (AIP, New York, 1985) p. 90.

[27] S. Karataglidis et al.,Phys. Rev C 61 (2000) 024319.

[28] J. S. Al-Khalili and J. A. Tostevin Phys. Rev. C 57 (1998) 1846.

[29] K. Arai et al., Phys. Rev. C59 (1999) 1432.

[30] V. Lapoux et al., in preparation.

[31] A. Pakou et al., submitted for publication

2 FIGURE CAPTIONS

Fig. 1

JLM angular distribution calculations for ^{6}He(p,p)^{6}He elastic scattering using the following densities: a) The shell model density of Karataglidis et al.[27]; b) The cluster model density of the Surrey group [28]; c) The cluster model density of Arai, Suzuki and Lovas [29]. In this last case the four different descriptions listed in Table 2 provide angular distributions which are exactly identical within the line width. Solid lines correspond to the best fit. Dashed lines correspond to the constrained fit (see Table 2 and text).

Fig. 2

a): JLM angular distribution calculations for the ^{6}He(p,n)^{6}Li$^{*}_{(3.56MeV)}$ reaction. The dashed, solid and dashed-dotted lines correspond to an isovector normalization of λ_{isov}=1.0, 1.4 and 1.8 respectively.

b): JLM angular distribution calculations for the ^{6}He(p,n)^{6}Li elastic scattering for three different density distributions. The solid line corresponds to the shell model density [27], the dashed line to the three-body cluster model of the Surrey group [28], the dotted line to the Arai–Suzuki–Lovas cluster model [29]. The adopted optical potential normalization factors are those obtained via the constrained fit (Table 2). The isovector normalization factor is 1.4.

$\lambda_v(\lambda_w$=0.8)	σ_R(mb)	λ_w (λ_v=1.0)	λ_{isov}=1.4 σ_R(mb)	λ_{isov}=1.0 σ_R(mb)
1	397	1	451	424
0.9	393	0.9	425	399
0.8	388	0.8	397	372
0.7	383	0.7	365	341
0.6	378	0.6	330	307

TABLE 1. Reaction cross section as a function of the normalization factors for the real and imaginary JLM potential, λ_v and λ_w. For the first set of calculations (first two columns), λ_w is fixed to the standard value of 0.8, and λ_{isov}=1.0. For the second set of calculations (last three columns), λ_v is fixed to the standard value of 1. The calculations including a variation in the imaginary potential are performed for two values of the isovector normalization, λ_{isov}=1.4 and 1.0. The ^{6}He density distribution from the shell model [27] is used.

density	$r_m(fm)$	$r_p(fm)$	$r_n(fm)$	λ_v	λ_w	χ^2	σ_R(mb)
A	2.52	2.03	2.73	0.85	0.59	1.12	320
				0.88	0.85	3.96	407
B	2.53	1.94	2.78	0.87	0.66	0.90	337
				0.9	0.88	2.65	406
C-a	2.49	1.82	2.77	0.88	0.74	0.85	353
				0.89	0.92	2.20	407
C-b	2.42	1.81	2.68	0.88	0.75	0.80	351
				0.89	0.92	2.22	407
C-c	2.34	1.75	2.59	0.88	0.85	0.85	365
				0.89	1.0	2.10	404
C-d	2.33	1.76	2.57	0.88	0.84	0.84	364
				0.89	1.0	2.13	406

TABLE 2. Details of the densities used in the JLM calculations and the potential renormalizations (λ_v, λ_w) used to fit the elastic angular distributions. The density indices indicate (A) shell model densities from Karataglidis-Amos[27]; (B) three-body cluster model of ref. [28]; (C) three-body cluster model of Arai-Suzuki-Lovas [29] (C-a: a pure three-cluster α+n+n model ; C-b: a pure three-cluster model with a t+t component; C-c: an extended three-cluster [3N+N]+n+n model; C-d. an extended three cluster model with a t+t component). The RMS radii for the matter, proton and neutron distributions are given. For each density, the first line indicates the best fit results, varying both λ_v and λ_w and the second line corresponds to constrained fit, where the imaginary part was set to a value such as to reproduce the reaction cross section results (λ_{isov}=1.4 in both cases)

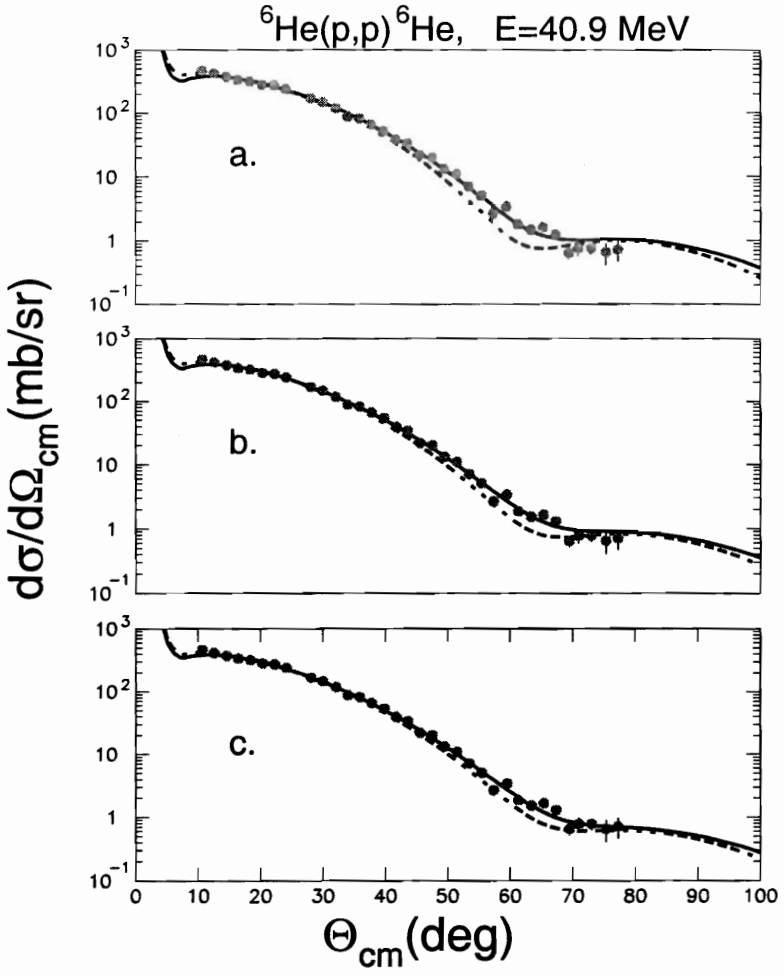

Fig. 1

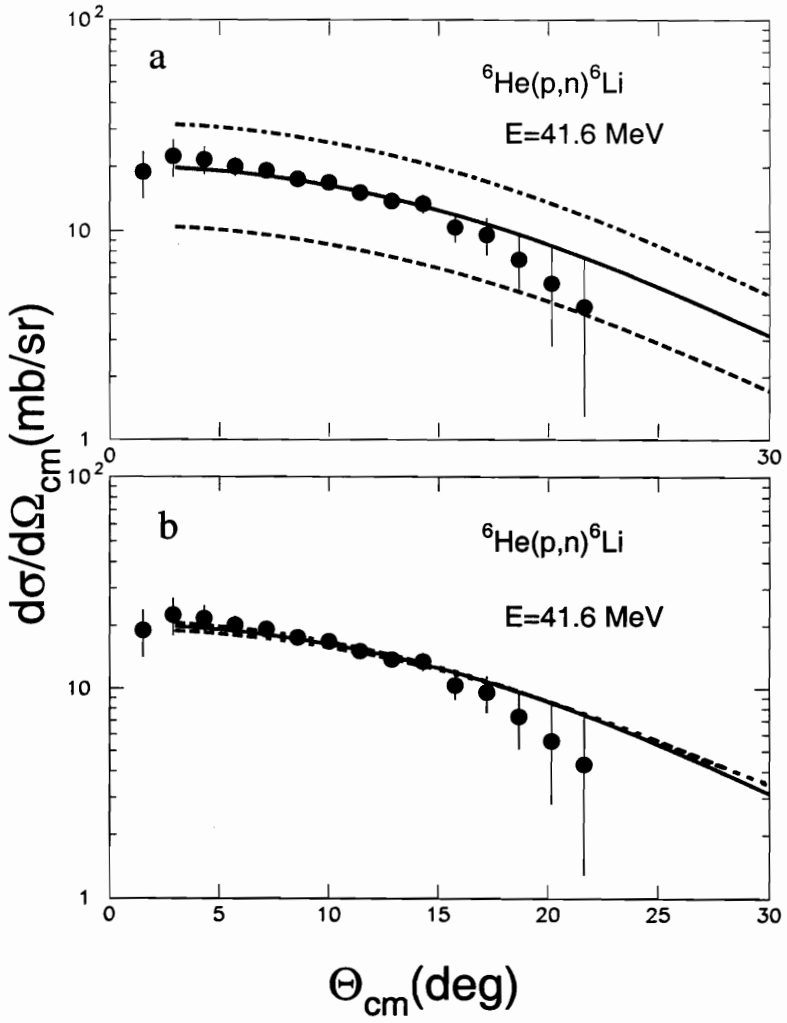

Fig. 2